ABSTRACT

EXPERIMENTAL STUDY OF IGNITION OF MECHANICAL ALLOY AND PURE METAL POWDERS

by
Ruslan S. Mudryy

Mechanical alloys of Al-Mg, Al-Zr, Al-Ti, Al-Li, Al-C, Al-Mg-H, B-Mg, B-Al, and B-Ti were produced and tested for possible applications as high energy density additives to fuels, propellants, explosives, and incendiaries. These new materials are metastable, supersaturated, nanocrystalline solid solutions that include a base metal as a solvent and another component (metal or gas, e.g. hydrogen) as a solute. Phase changes occurring in such materials during ignition and combustion are expected to significantly affect both ignition and burn rates. This experimental program focused on the characterization of ignition kinetics of these alloys. An experimental setup is built around an electrically heated filament coated with the powder of a tested material. The filament is heated at a reproducible rate causing ignition of the powder. The temperature of the filament at the instant of ignition is measured using an optical pyrometer. The time of ignition and the filament heating rate are determined from the optical and electric signals recorded using a computerized data acquisition system. For alloys with higher ignition temperatures, video imaging and image processing technique was used. Experiments showed that the pyrometer technique is more accurate but a discrepancy between the video-imaging and pyrometry is small. Each material is ignited at three different heating rates. Ignition temperatures are determined for aluminum and boron-based alloys as a function of their elemental composition. It is observed that the ignition temperatures of a set of prepared aluminum-based alloys are significantly lower than that of the pure aluminum. It was

also found that the measured ignition temperatures increased with an increase of heating rate for all the investigated alloys.

EXPERIMENTAL STUDY OF IGNITION OF MECHANICAL ALLOY AND PURE METAL POWDERS

by
Ruslan Mudryy

A Dissertation
Submitted to the Faculty of
New Jersey Institute of Technology
In Partial Fulfillment of the Requirements for the
Degree of Master of Science in Mechanical Engineering

Department of Mechanical Engineering

May 2003

APPROVAL PAGE

EXPERIMENTAL STUDY OF IGNITION OF MECHANICAL ALLOY AND PURE METAL POWDERS

Ruslan Mudryy

Dr. Edward L. Dreizin, Dissertation Advisor — Date
Associate Professor of Mechanical Engineering, NJIT

Dr. Boris Khusid, Committee Member — Date
Associate Professor of Mechanical Engineering, NJIT

Dr. Chao Zhu, Committee Member — Date
Assistant Professor of Mechanical Engineering, NJIT

BIOGRAPHICAL SKETCH

Author: Ruslan Mudryy

Degree: Master of Science

Date: December 2002

Undergraduate and Graduate Education:

- Master of Science in Mechanical Engineering,
  New Jersey Institute of Technology, Newark, NJ, 2003

- Master of Science in Applied Physics,
  Lviv National University by Ivan Franko, Lviv, Ukraine, 1994

- Bachelor of Science in Applied Physics,
  Lviv National University by Ivan Franko, Lviv, Ukraine, 1992

Major: Mechanical Engineering

Presentations and Publications:

Dreizin E., L., Shoshin Y.L., Mudryy R.S., Constant pressure flames of aluminum and aluminum-magnesium mechanical alloy aerosols in microgravity, *Combustion and Flame* 130:381-385, (2002).

Shoshin Y.L., Mudryy R.S., and Dreizin E.L., Preparation and Characterization of Energetic Al-Mg mechanical alloy powders, *Combustion and Flame* 128:259-269, (2002).

R. Mudryy, P. Singh and A. D. Rosato, Air Entrainment and Segregation in Powder Flows, *Segregation in Granular Flows* (eds. A. D. Rosato and D. L. Blackmore), 327-336, Kluwer, Dordrecht, (2000).

P. Singh, T.K.S. Solanky, R. Mudryy, R. Pfeffer and R. N. Dave, Estimation of Coating Time in the Magnetically Assisted Impaction Coating Process, *Powder Technology*, vol. 121, No. 2-3, 159-167, (2001).

Holovko M.F., Mudry R.S. The associative effects in dipole systems: Influence on critical behaviour, *Ukr. Phys. Journ.*, vol. 45, No. 1, 112-117, (2000).

To my beloved family

ACKNOWLEDGMENT

I would like to express my deepest appreciation to Dr. Edward Dreizin, who not only served as my research supervisor, providing valuable and countless resources, insight, and intuition, but also constantly gave me support, encouragement, and reassurance. Special thanks are given to Dr. Boris Khusid and Dr. Chao Zhu for actively participating in my committee.

Many of my fellow graduate students in the Energetic Materials Research Laboratory are deserving of recognition for their support. I also wish to thank Dr. Yu. Shoshin for his assistance.

TABLE OF CONTENTS

TABLE OF CONTENTS
(Continued)

LIST OF TABLES

LIST OF FIGURES

LIST OF FIGURES
(Continued)

CHAPTER 1
INTRODUCTION

1. 1 Objective

The objective of this research is to investigate experimentally ignition of mechanical alloyed metal powders designed for this project and reference samples of pure metal powders. Ignition experiments were conducted using an optical pyrometry and video image processing techniques. A range of mechanical alloys including Al-Mg, Al-Ti, Al-Li, B-Ti, Al-Zr, Al-C were investigated. Dependency of ignition temperature on heating rate and alloy composition was investigated.

1.2 Background Information

High energy density materials (HEDM) are the elements and compounds with high combustion enthalpies. HEDM are used as propellants in many space exploration and military systems, such as rockets, missiles, guns, and pressure generators. Metals are widely used in contemporary energetic formulations because of their very high volumetric and gravimetric combustion enthalpies [Dreizin, 2000]. However, high temperatures of ignition and slow burning rates do not allow one to fully exploit metals' great potential as high enthalpy fuels.

Using a new concept taking advantage of internal phase changes [Dreizin et al., 1999] to enhance metal ignition and combustion, supersaturated solid solutions that include base metal as a solvent and another component as a solute have been recently produced by mechanical alloying (MA) [Shoshin et al., 2002]. Two main groups of supersaturated solid solutions were prepared and investigated. The first one includes

aluminum based binary systems with such solute elements as Mg, Li, Zr, C, and MgH_2. The second group includes boron based binary systems with Ti, Mg, and Al added as a solute. Properties of the prepared alloys vary depending on the solute content. Ignition behavior of new materials has been tested as described and discussed in the following sections.

CHAPTER 2

EXPERIMENTAL SETUP

Investigated alloy powders were deposited on filaments, which were later electrically heated in room air. A schematic diagram of the experimental setup is shown in Figure 2.1. Filament length was approximately 40-45 mm and only a small portion of the filament (3-4mm) was coated with the alloy powder. A car battery was used as a DC power supply. A resistance box connected in series with the filament provided an opportunity to vary the heating rate. The temperature of the filament adjacent to the coated portion was optically monitored using a high-speed infrared pyrometer (OS1532 by Omega Engineering) and, in different experiments, with a 3 CCD digital video camera (Panasonic AG-EZ30P). The filament was heated at a reproducible rates varied from 175 K/s to 5100 K/s and filament temperature at the instant of the powder ignition was determined. A moment of ignition was determined using a photodiode focused at the powder coating. Both photodiode and pyrometer were connected to a PC data acquisition system. A Scope card 220 hardware and software package (Hung Chang Co.) were used respectively to produce and analyze the output of the data acquisition system. Heating rate, ignition temperature and ignition time were determined from the recorded data.

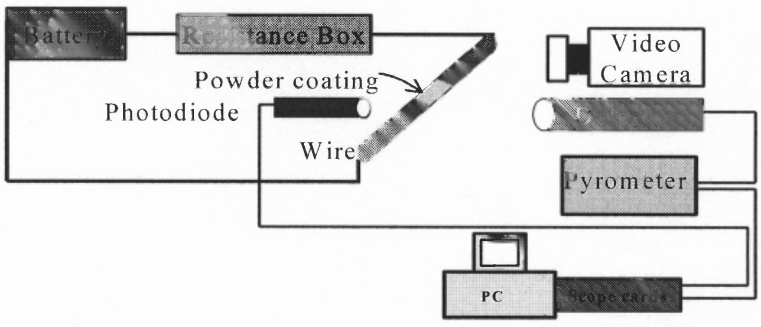

Figure 2.1 Experimental setup for ignition tests.

2.1 Heated Filament Holders

During the heating, a filament held at its ends elongates, bends, and moves away from the pyrometer focus. It results in inaccurate temperature measurements. This problem was circumvented using a specially designed filament holder. Two ends of the filament were attached to two metal brackets, as shown in Figure 2.2. One of the brackets was mounted on a linear slide and attached to a spring. The second end of the spring was attached to a flange, so that the heated filament was continuously stretched during the experiment. In some experiments, when a high heating rate was desired, the filament could heat up to a temperature exceeding the material melting point. In such experiments, the filament was broken during the heating, but, usually, after the ignition of the alloy sample.

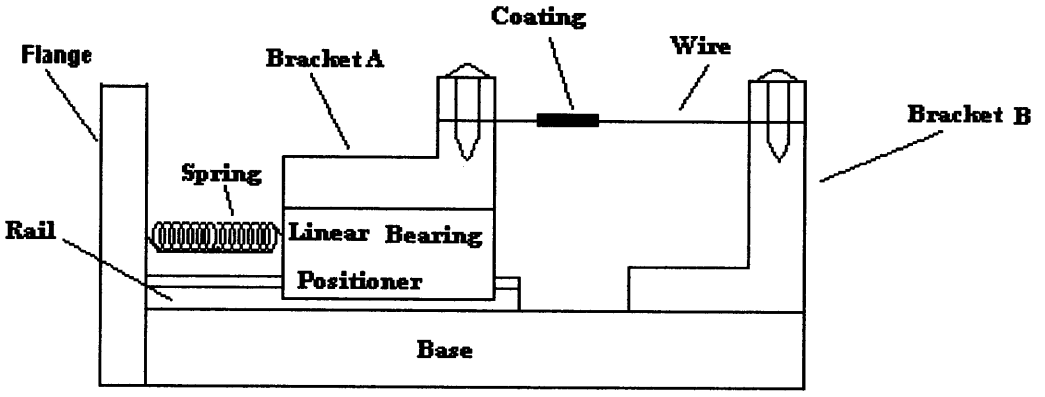

Figure 2.2 Schematic diagram of a heated filament holder.

2.2 Filament Types

Two different types of filaments were used in this study for ignition experiments. For most alloys, a wire composed of 60% nickel, 16% chromium and 24% iron was used. For alloys with the ignition temperature higher than 1300 K (e.g., 10%Ti-90Al%, 10%C-90%Al and 10%Zr-90%Al), a thin graphite rod was used as a more refractory filament.

Table 2.1 Filament Characteristics

Filaments	Diameter, mm	Emissivity coefficient, %
Nickel-Chromium wire	0.48	38 [Weast, 1981]
Fine Graphite rod	0.50	95 [Weast, 1981]

CHAPTER 3

METHODS OF THE IGNITION TEMPERATURE MEASUREMENT

3.1 Video Technique

A video signal from a camera used to monitor the ignition event was transferred to a PC. A Video Capture 6.0 software was used to measure the radiation intensity of the filament prior to ignition. The ignition of the powder was accompanied by a bright flash resulting in the saturation of the video camera. A set of sequential frames during the heating of a coated filament is presented in Figure 3.1. The frame at t=2.76 s in Figure 3.1 corresponds to the last pre-ignition moment, detected by the camera.

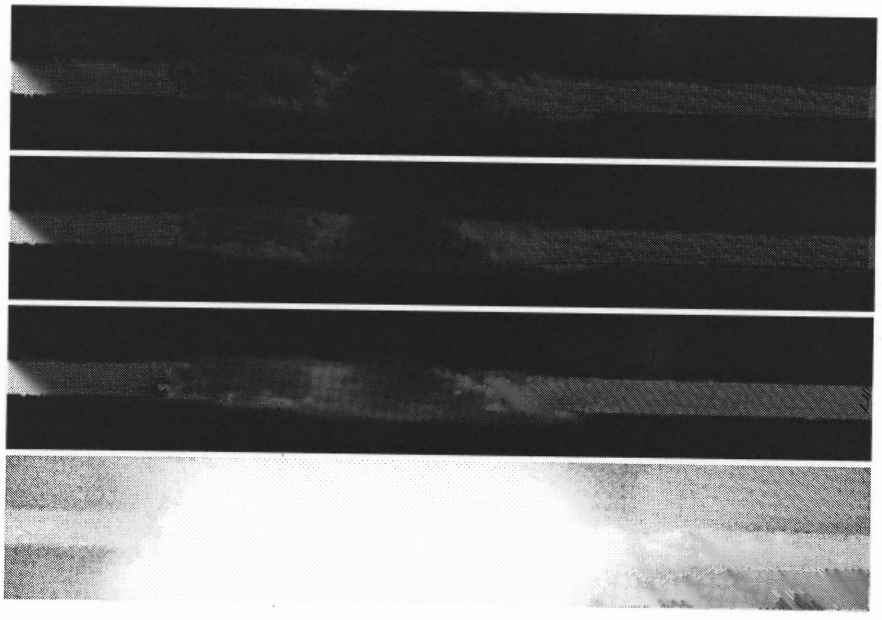

Figure 3.1 A video frame sequence showing an ignition of 40%Mg-60%Al alloy. The time markers show the time from the beginning of the filament heating.

To avoid possible errors due to different and unknown emissivities of alloys the radiation from the wire surface radiation was monitored to determine the ignition temperature, as opposed to the radiation of the powder surface.

Different aperture/exposure settings of the video camera were used for the recording of ignition for different alloys, but the distance between camera's objective and filmed object of interest was always the same (160 mm). For each specific setting, the camera was calibrated using a NIST certified strip lamp. A strip lamp filament was filmed from the same distance as the alloy-coated filament. Digital images were transferred to a PC and processed by Video Capture 6.0 software. Area normalized radiation intensities were determined for each image. About 3000 pixels were used for each analyzed image to determine the average radiation intensity. In addition, radiation intensities of color components (red, green and blue) were determined because the average radiation intensity could exceed the saturation limit of the video camera at some temperature. Fifteen calibration points (images of the strip lamp at different temperatures) were used in the temperature range from 900 K to 2400 K. To determine the strip lamp filament's temperature, the calibration curve shown in Figure 3.2 and supplied with the lamp was used (see Figure 3.2). The electric current through the strip lamp was measured by a Radio Shack 22-163 digital multimeter using a shunt.

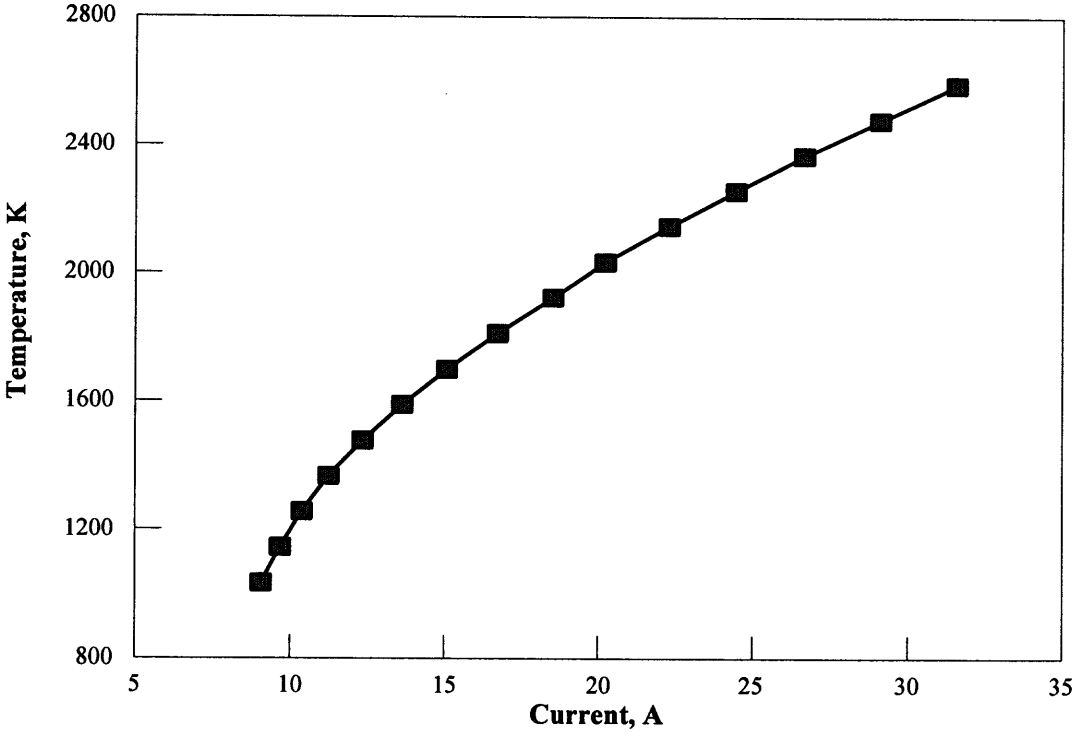

Figure 3.2 Dependence of a strip lamp filament temperature on electric current.

Using the processed data, the dependence of the strip lamp filament radiation temperature on the radiation intensity of color components (except for the blue component, which was very week for this video camera setting) and on the average radiation intensity were plotted as presented in Figure 3.3. It is an example of calibration curve obtained for camera exposure of 1/250 s, and camera aperture of 28 dB. Most of the investigated alloys ignited at a temperature range where the green component of the radiation intensity was convenient to measure, was always detectable and was not saturated for the most cases of the video camera setting (see Figure 3.4). The calibration curves, shown in Figure 3.4, were exploited to determine the ignition temperatures of alloys using video-imaging.

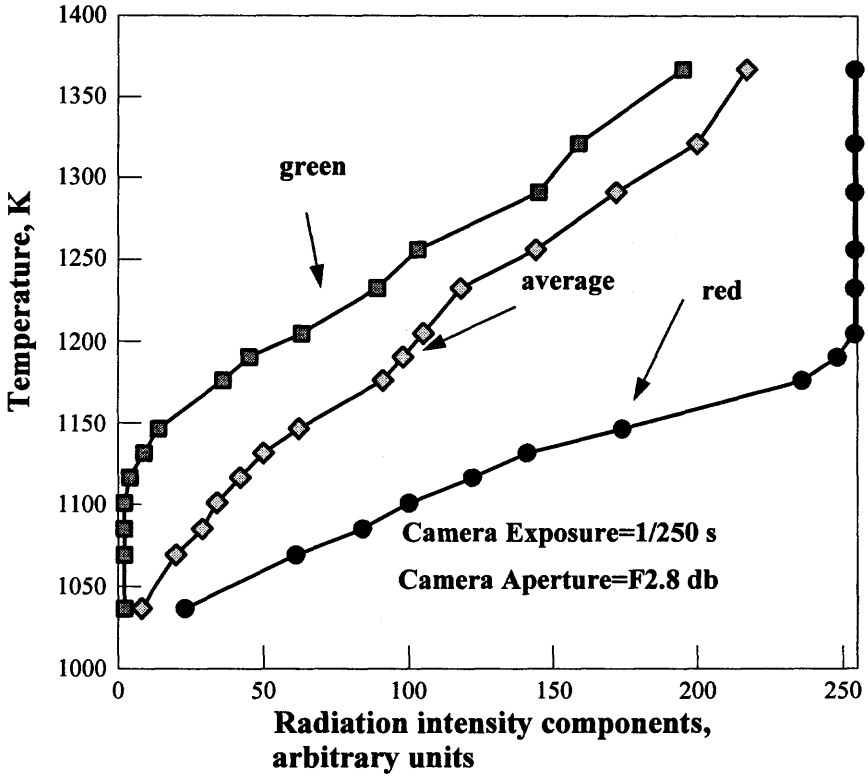

Figure 3.3 Radiation temperature as function of radiation intensity components and average radiation intensity.

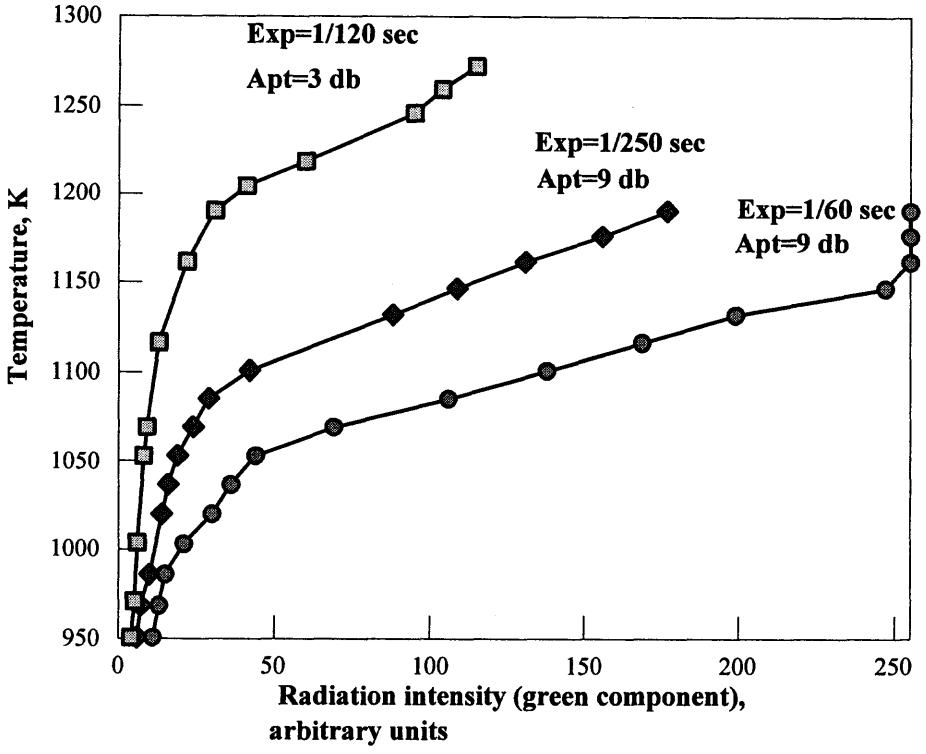

Figure 3.4 Radiation temperature as a function of green radiation intensity component at different video camera settings.

3.2 Pyrometer Technique

3.2.1 Measurements

Radiation emitted by a heated filament was collected by a pyrometer detector focused on filament. An interconnecting fiber optics cable carries the optical signal from the detector head to the main pyrometer unit (Figure 2.1). Coefficient of emisivity for the filament was pre-set on the front panel of the pyrometer. The measured temperature is displayed by a digital display, a voltage proportional to the temperature is also formed at an output of the data acquisition system. The data acquisition recorded the temperature trace as a function of time. To convert the pyrometer output voltage to the temperature units (K), the calibration was performed using a BB-4 blackbody radiation source by Omega

Engineering. The source provides a stable blackbody radiation preset for the temperatures into range of 400 F to 2000 F (478 K to1367K). The radiation of the black body source was measured by the pyrometer at several different temperatures to obtain a calibration plot for the data acquisition. Acquisition card software recorded data in arbitrary units and the transformation to voltage was performed using additional calibration that provides analytical expression of voltage as function of data acquisition units. Temperature as function of voltage for scope card sensitivity of 0.2V per division is shown in Figure 3.5. At low temperature (730K and less) pyrometer output signal has a different slope of temperature-voltage dependence.

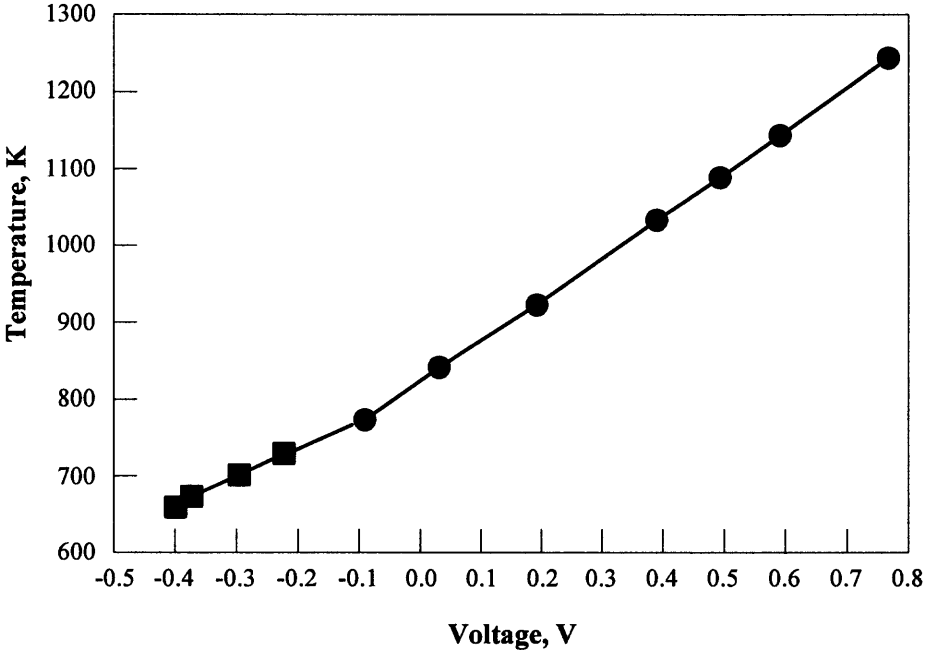

Figure 3.5 Radiation temperature measured by the pyrometer as a function of the pyrometer output voltage (for scope card sensitivity of 0.2V per division).

An analytical equations for this linear calibration curves are:

$$Temperature(K) = 389.11 \times Voltage(V) + 816.34 \quad \text{(for temperatures< 730K)}$$

$$Temperature(K) = 547.45 \times Voltage(V) + 821.31 \quad \text{(for temperatures>774K)}$$

Analytical equation for (730-774K) temperature range within was derived using coordinates of border points.

$Temperature(K) = 331.34 \times Voltage(V) + 803.152$ (for temperatures<774K and >730K)

Different scope card sensitivity setting produced different transformation coefficients of input voltage to recorded outcome expressed arbitrary units. The equations for different scope card sensitivity settings are presented in Appendix A. Thus, all the experimental data obtained with the PC acquisition system were converted into temperature units (K).

3.2.2 Pyrometer Focusing

To measure the ignition temperature of alloys, the pyrometer was focused on a spot of the filament adjacent to the powder coating. The measurement of filament temperature rather then powder coating temperature eliminated uncertainty associated with different emissivity coefficients for different alloys. It introduced some, smaller, uncertainty in ignition temperature of powder as temperature of wire not the temperature of powder was directly measured. For repeatable pyrometer focusing, a high intensity light source, OS1500-BLS by Omega Engineering was used. The detector's fiber cable was removed from its receptacle in the pyrometer and inserted into an output of the light source. The detector head also served as a focusing lens so an illuminated target spot was projected on the filament. The pyrometer was considered well focused if the spot size was equal to ≈ 0.3 mm. The respective distance between the detector head and the target spot was equal to ≈ 25 mm.

3.2.3 Investigation of a Temperature Gradient Along the Wire

As noted above, to avoid the effect of unknown powder emissivity, the pyrometer was always focused at a spot adjacent to the coated region. The distance from the pyrometer focal point to the coating was about 2 mm. The temperature gradient along the filament could develop during the heating and could affect the measurements and their interpretation. To evaluate possible error caused by the temperature gradients the temperature measurements were made at three different positions along the filament (3 mm from one another). The result showed that the difference was reasonably small (Table 3.1).

Table 3.1 Temperature of Nickel –Chromium Filament at Different Positions During the Heating Time

Heating time, sec	Left position temperature, K	Central position temperature, K	Right position temperature, K
2	699	712	712
3	855	861	864
4	948	957	967

Thus, it is proved that the temperature of filament measured 3 mm away from the powder was reasonably close ≈ 10K to the temperature of the filament under the alloy coating.

3.2.4 Use of Photodiode

A photodiode was utilized to determine a moment of ignition. The photodiode was focused on the powder coating. The photodiode signal was transmitted to the PC based data acquisition system. When ignition occurred, a fast increase of the photodiode curve amplitude (an abrupt peak) was observed. The moment corresponding to the peak onset is

defined as the moment of ignition. The temperature of ignition was determined from the pyrometer output signal at this particular moment as shown in Figure 3.6.

3.2.5 Determination of the Ignition Moment

To find the ignition temperature, it is necessary to clearly identify the ignition moment on the photodiode curve. Two different methods were used to define the ignition moment and consequently, the ignition temperature. In the first method, the sharp increase on the photodiode curve was identified based on the visual inspection of the recorded curves (Figure 3.7).

In the second method, the temperature at the end of a pre-ignition period was approximated by a straight line. The time period for this linear approximation was chosen to be long enough to be sure that the temperature of powder changed but the influence of the exponential Arrhenius contribution from the chemical reaction was still negligible. Ignition peaks on the photodiode signal were observed in all of the ignition experiments. The width of the peaks shows a characteristic time of the ignition event. For practical purposes, the pre-ignition periods considered to produce the linear fit were at least 5 times longer then that characteristic time. Thus, for Al-Mg system (presented in Figures. 3.6-3.8) this approach indicated that about 0.5 s period is sufficient for reasonable linear approximation of the emission signal during the final portion of pre-ignition periods.
The second straight line approximated the time dependence of the photodiode signal after the ignition peak onset. The moment at which the two lines crossed was defined as the ignition time.

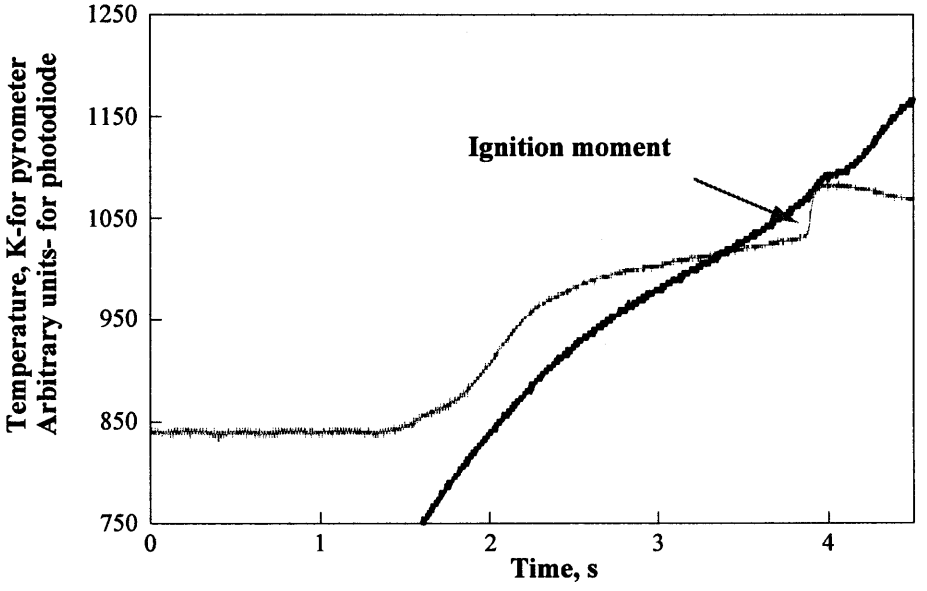

Figure 3.6 Recorded filament temperature as a function of the heating time and a respective photodiode trace.

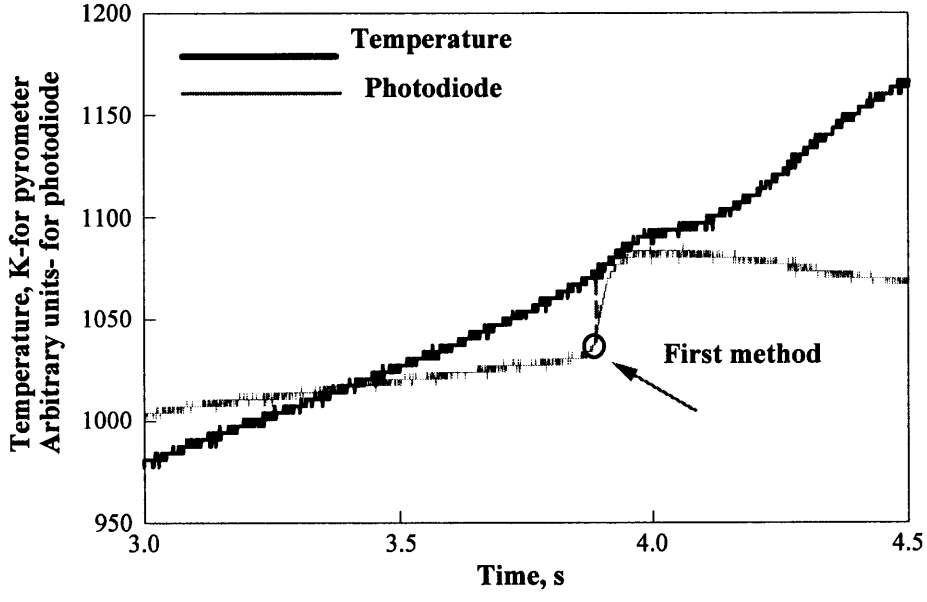

Figure 3.7 Alloy ignition temperature determined by the first method.

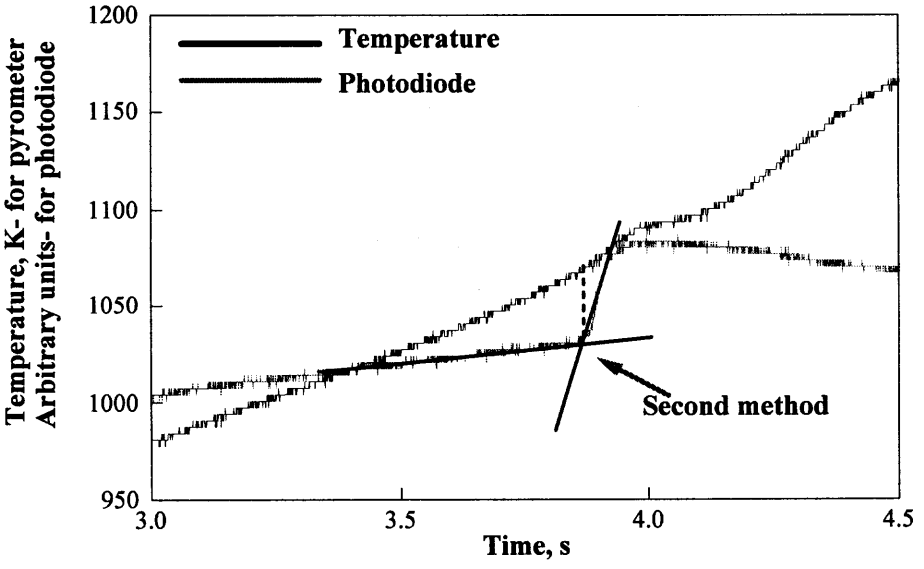

Figure 3.8 Alloy ignition temperature determined by the second method.

3.3 Comparison of Ignition Temperatures Obtained by the Video and Pyrometer Techniques

The ignition temperature of a selected alloy (40%Mg-60%Al) was measured by the pyrometer and at the same time, the ignition process was recorded with the video camera. Obtained results (Figure 3.9) show that the difference between the two techniques is statistically insignificant. For nine experimental runs the average ignition temperature, measured by the video technique is 1003 K and it is 990 K as measured by the pyrometer technique. Thus, both techniques were considered as adequate for the ignition temperature measurements.

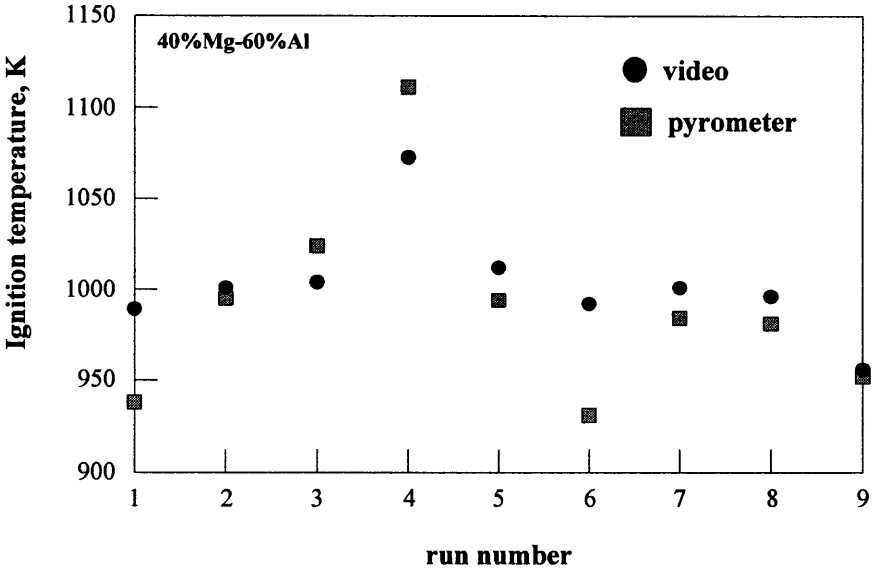

Figure 3.9 Ignition temperatures of a 40%Mg-60%Al alloy obtained by both video and pyrometer techniques for the same ignition event.

CHAPTER 4

POWDER COATING PROCEDURES APPLIED TO DIFFERENT SUBSTRATES

4.1 Nickel-Chromium Wire

Nickel-Chromium wire was stretched manually before each experimental run to keep the pyrometer well focused on the filament during the heating. An alloy powder was mixed with a liquid and then a small quantity of this mixture was applied to the filament using a brush. The coating was dried using a fan. The type of the liquid used depends on the alloy system. For the Al-Mg system, tap water was adequate, but Al-Li and Ti-B alloy systems were observed to chemically react with water. Ethanol denaturated (CH_3CH_2OH) was used for the Ti-B system. Al-Li alloys were coated with liquid hydrocarbon, Ronsonol Lighter Fluid synthesized from naphta, because even a small amount of water contained in alcohol could react with lithium. After drying using an electric fan, liquid was expected to evaporate completely and was not expected to affect the ignition temperature of the coated alloy.

Several experimental runs were performed to determine whether any difference could be detected in the ignition temperature of the same powder deposited using hydrocarbon and alcohol as liquids. Relatively close ignition temperatures of a 30%Ti-70%B alloy were observed for the two liquids: for alcohol, the average temperature is T=717K, (s.d.=18) and for hydrocarbon, the average temperature is T=698K (s.d.=23).

4.2. Thin Graphite Rod

It was observed that some of the alloy powders coated on the filament fell off the filament upon the filament heating. Ignition temperature of such alloys was usually high and thin graphite rods were used as a filament. To keep the powder sitting on the rod during the heating, small quantity (1 drop per cubic centimeter) of Pentel glue was mixed with water and used as liquid. Ti- Al alloy system was tested to see whether the glue affected the ignition temperature. An alloy sample (25%Ti-75%Al), which is possible to ignite without the glue, was selected for these tests. Obtained result showed that there was a significant difference between the case with and without glue. The average ignition temperature for the case with pure water was 863K and for the water with glue the temperature was 782K. Ignition of the same powder following to the same coating procedure was also performed on a Nickel-Chromium wire. For the powder on wire, the ignition temperature for initial water suspension was T=808K (s.d.=6K) and for initial water and glue suspension was T=811K (s.d.=15K). Probably, glue additive changes a heat transfer transition between graphite rod and alloy particle and it causes an effect in the ignition temperature of alloy. Therefore, additional experiments need to be conducted for investigation of heat transfer process.

Also, a noticeable discrepancy observed between the ignition temperatures of the same alloy on different filaments was most likely caused by the different heating rates applied.

CHAPTER 5

RESULTS SUMMARY

5.1 Ignition Temperatures for Al-Mg Alloys at Different Heating Rates

According to the described above methodology, Al-Mg alloy powders (from 10 to 50% of magnesium content) mixed with water were placed on a round Ni-Cr wire (0.48mm diameter) and dried. Ignition temperatures were measured by pyrometer at three different heating rates (R=175 ± 40 K/s, 1300 ± 100 K/s and 5100 ± 740 K/s). The heating rates were estimated based on the time required to achieve the ignition temperature starting from 775K. Pyrometer has linear output signal from this temperature.

There was a small difference in the heating rates for similar experimental conditions because a car battery was charged to a somewhat different level.

Ignition of each composition was observed ten times under similar conditions and the average ignition temperature and standard deviation were calculated. Techniques for finding ignition temperature using both pyrometer and photodiode traces, as described in Section 3.2.5, were used. Figure 5.1 represents typical ignition curves for a set of 10 runs for each alloy composition (except for the 10Mg-90Al alloy, that was not possible to ignite) at a heating rate of R=175 ± 40 K/s. Ignition peaks on the photodiode traces are clearly visible. Ignition temperatures determined by the two methods are shown in Table 5.1 (ref. Section 3.2.5).

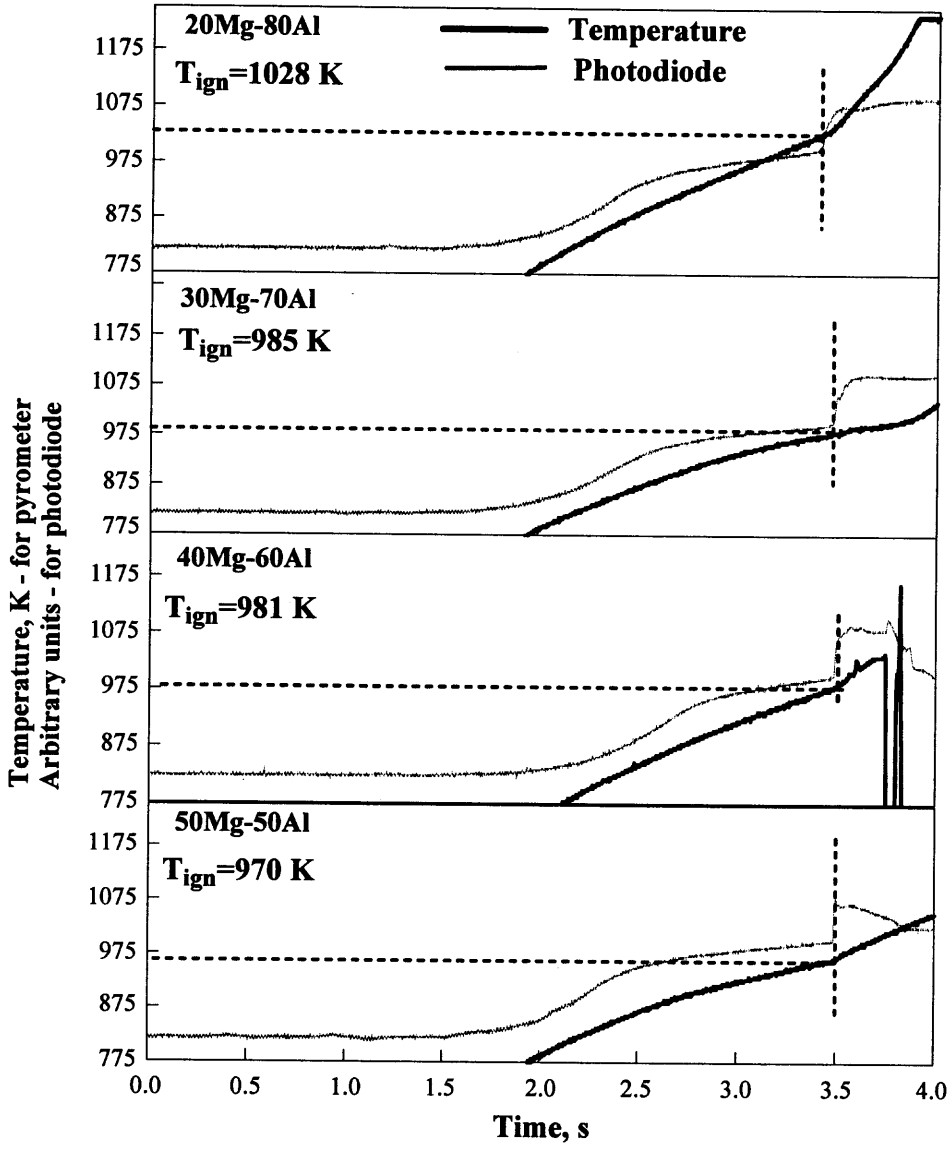

Figure 5.1 Temperature and the photodiode traces as a function of the heating time at a heating rate R=175 ± 40 K/s for Al-Mg alloys.

Table 5.1 Ignition Temperatures Determined by Two Methods, Described in Section 3.2.5 at a Heating Rate R=175 ± 40 K/s for Al-Mg Alloys (10 repeats for each alloy)

Alloy	Ignition temperature, determined by 1-st method, K	Ignition temperature, determined by 2-nd method, K
20Mg-80Al	1020 ± 36	1018 ± 36
30Mg-70Al	976 ± 32	976 ± 32
40Mg-60Al	970 ± 36	969 ± 36
50Mg-50Al	967 ± 54	967 ± 54

At higher heating rate R=1300 ± 100 K/s, 10Mg-90Al alloy powder was ignited as well as other alloys, but the radiation intensity of the ignition peak was small (Figure 5.2).

Calculated average ignition temperatures are shown in Table 5.2.

Table 5.2 Ignition Temperatures Determined by Two Methods, Described in Section 3.2.5 at a Heating Rate R=1300 ± 100 K/s for Al-Mg Alloys (10 repeats for each alloy)

Alloy	Ignition temperature, determined by 1-st method, K	Ignition temperature, determined by 2-nd method,
10Mg-90Al	1199 ± 21	1176 ± 14
20Mg-80Al	1146 ± 49	1139 ± 49
30Mg-70Al	1095 ± 60	1095 ± 62
40Mg-60Al	1015 ± 34	1015 ± 33
50Mg-50Mg	1041 ± 55	1041 ± 55

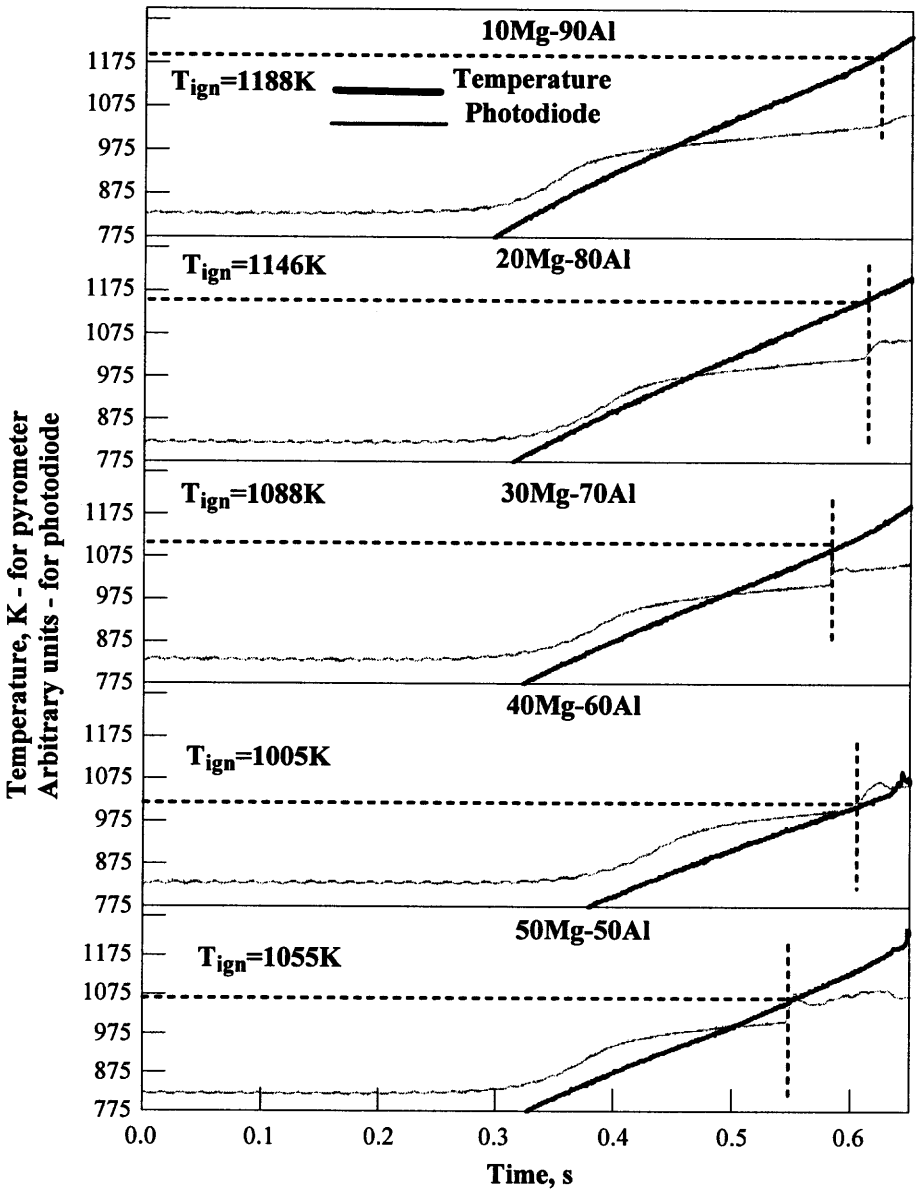

Figure 5.2 Temperature and the photodiode traces as a function of the heating time at a heating rate R=1300 ± 100 K/s for Al-Mg alloys.

At a heating rate R=5100 ± 740 K/s, ignitions of alloy powders with higher magnesium content were accompanied with bright flashes, which affected the pyrometer reading and resulted in additional peaks in the pyrometer temperature traces (e.g. Figure 5.3). However, the post-ignition peaks did not have an effect on the identified ignition temperatures. Results obtained by two methods are presented in Table 5.3

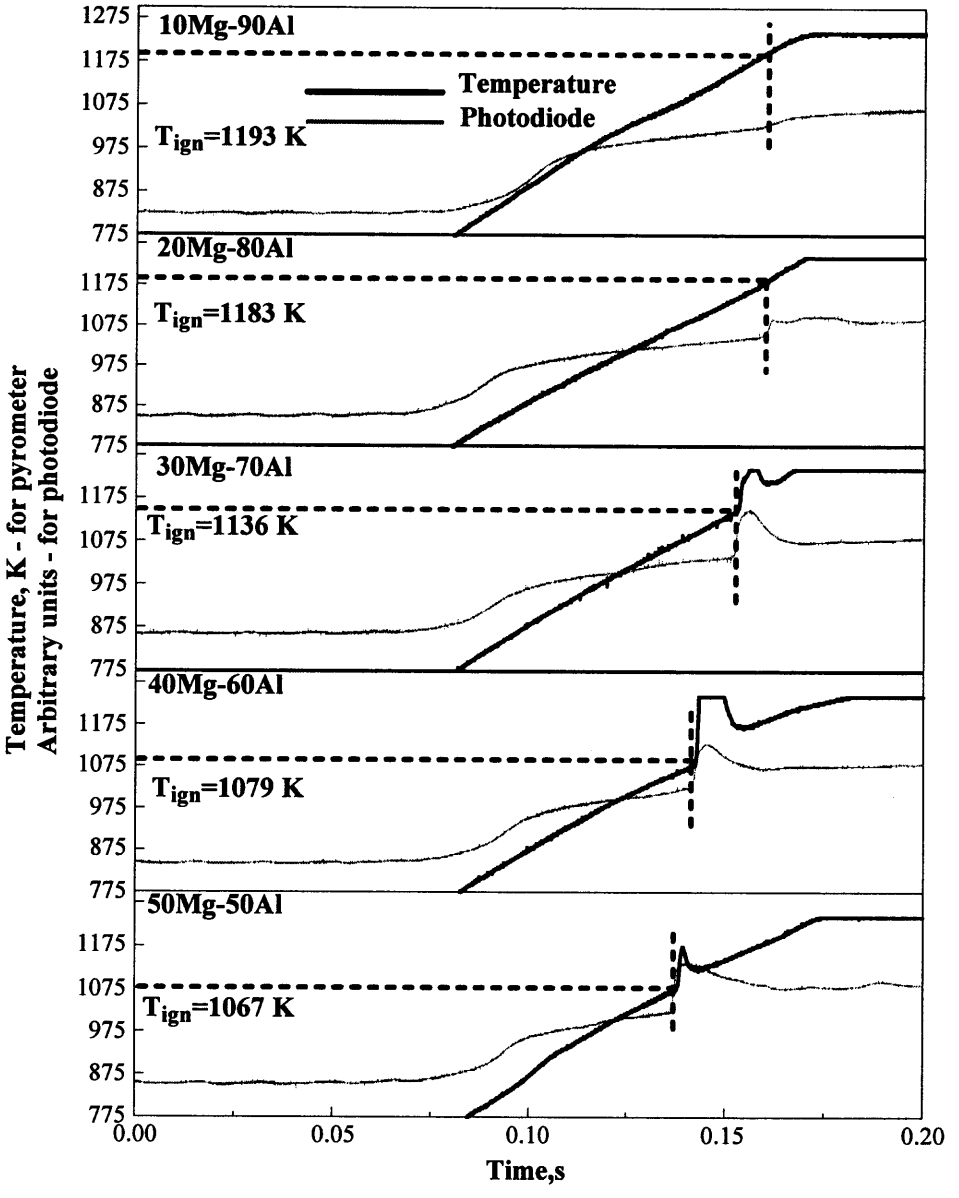

Figure 5.3 Temperature as a function of the heating time at R=5100 ± 740K/s heating rate for Al-Mg alloy system.

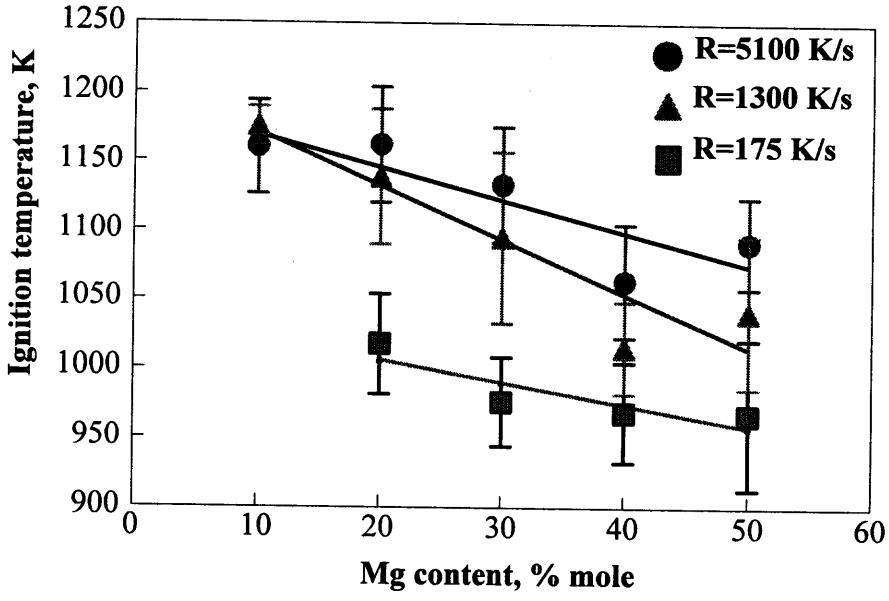

Figure 5.4 Ignition temperature of Al-Mg mechanical alloys at the average heating rates R=175 K/s, R=1300 K/s and R=5100 K/s.

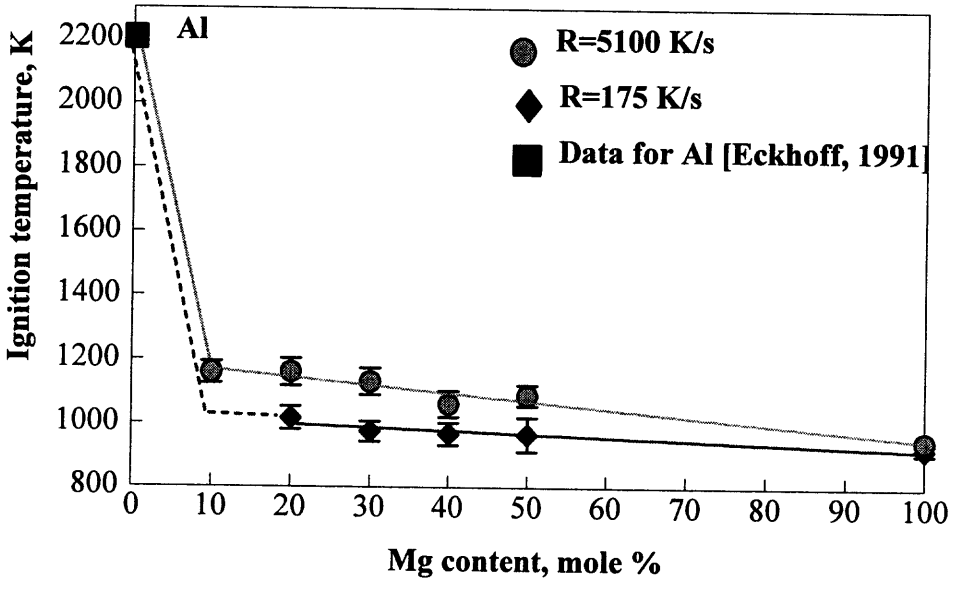

Figure 5.5 Ignition temperature as function of magnesium content in mechanical alloys at the average heating rates of R=175 K/s and R=5100 K/s. Aluminum ignition temperature is from Eckhoff, (1991).

Table 5.3 Ignition Temperatures Determined by Two Methods (Section 3.2.5) at a Heating Rate R=5100 ± 740 K/s for Al-Mg Alloys (10 repeats for each alloy)

Alloy	Ignition temperature, determined by 1-st method, K	Ignition temperature, determined by 2-nd method, K
10Mg-90Al	1163 ± 34	1160 ± 34
20Mg-80Al	1163 ± 43	1162 ± 42
30Mg-70Al	1134 ± 43	1133 ± 42
40Mg-60Al	1064 ± 41	1063 ± 41
50Mg-50Mg	1091 ± 32	1091 ± 33

Considering data shown in Tables 5.1-5.3, for it is clear that the two methods used for the temperature measurements gave very close results for Al-Mg system.

As was discussed above, at higher heating rates the ignition temperature of all alloys increased. An increase of the heating rate from R=175 ± 40 K/s to R=5100 ± 740 K/s resulted in an increase of the ignition temperature by approximately 150K, as shown in Figure 5.4

The ignition temperatures of Al-Mg alloys were found to be in a range, which was significantly lower than the ignition temperature of the pure Al. For the minimum heating rate case (R=175 ± 40 K/s) the difference was about 1300K (Figure 5.5) and for the maximum heating rate (R=5100 ± 740 K/s) the difference was around 1150K (Figure 5.5). These results have shown that lower ignition temperatures can be achieved for aluminum based mechanical alloys that can be beneficial for new HEDM.

5.2 Annealed Al-Mg Alloys

Ignition of HEDM usually depends on a number of experimental conditions, including the oxidizer composition, ambient pressure and temperature, and heating rate. In general, ignition can be influenced by metastable subsolidus reactions through energetic effects. Either the heat released in the relaxation of the metastable state triggers ignition directly, or boosts heating rates so that the point of ignition is reached faster. A rough estimate of expected heat effects in the present system can be obtained by comparing ignition temperatures of prepared alloys in metastable and stable states. Annealing technique was used to transfer alloys from metastable to the thermodynamically stable state. However, conducted experiments showed that there was almost no difference in the ignition temperatures for annealed and as-prepared, metastable alloys (Figure 5.6). A small difference between ignition temperatures was within the range of experimental errors. It is interesting that the "ignition peaks" observed for annealed alloy (Figure 5.7), appear to be weaker than similar peaks for the same composition "as prepared" alloys heated at the same rate, (Figure 5.2). Ignition temperatures determined from traces, e.g., Figure 5.7 using the two determination methods, described in Section 3.5.2, are also close to each other (Table 5. 4).

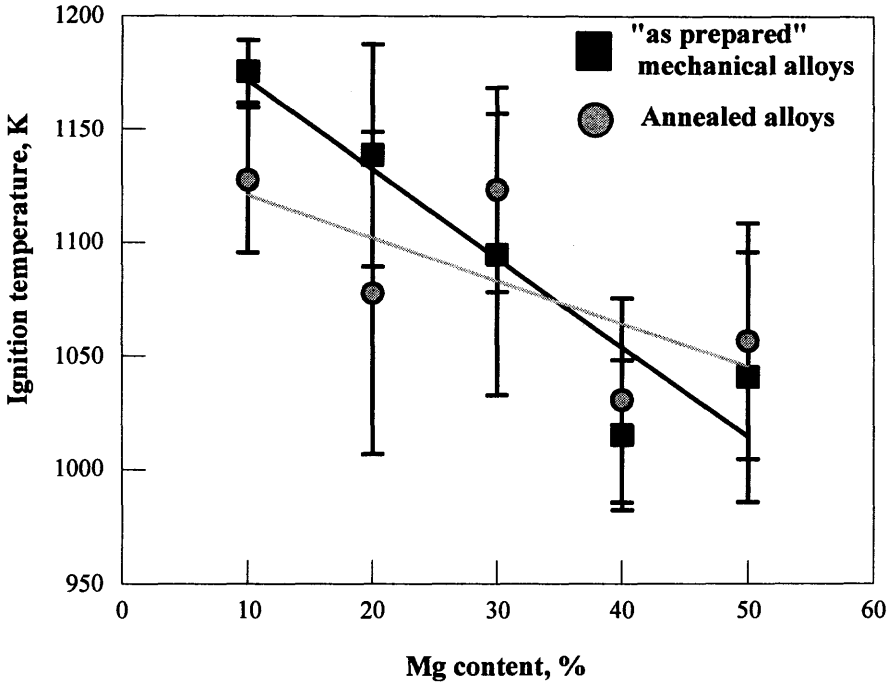

Figure 5.6 Temperature as a function of the magnesium content at R=1300 ± 100 K/s heating rate for Al-Mg annealed alloys.

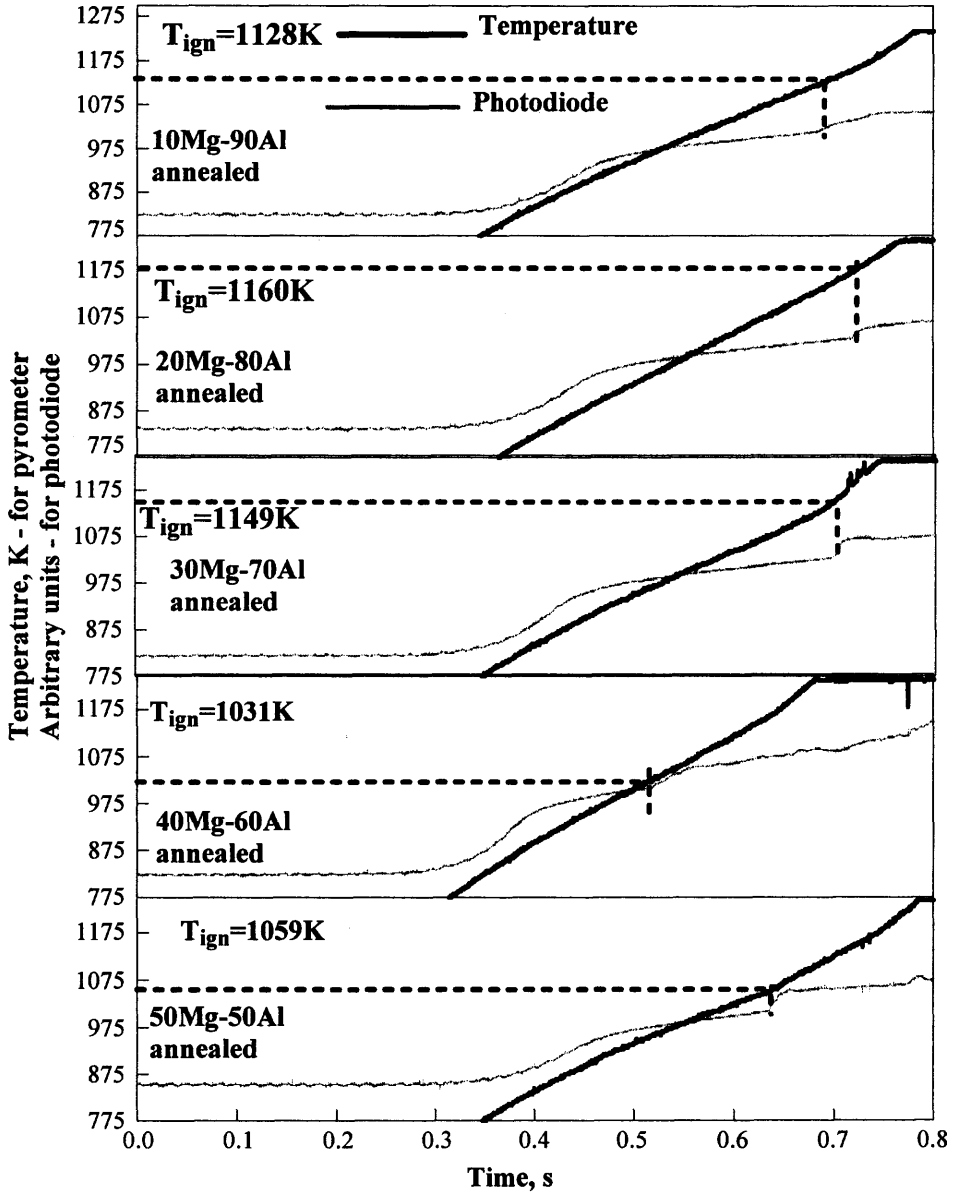

Figure 5.7 Temperature as a function of the heating time at a heating rate R=1300 ± 100 K/s for Al-Mg annealed alloys.

Table 5.4. Ignition Temperatures Determined by Two Methods Described in Chapter 3.5.2 at a Heating Rate R=1300 ± 100 K/s for Al-Mg Annealed Alloys (10 repeats for each alloy)

Annealed Alloys	Ignition temperature, determined by 1-st method, K	Ignition temperature, determined by 2-nd method, K
10Mg-90Al	1134 ± 35	1128 ± 32
20Mg-80Al	1081 ± 82	1078 ± 84
30Mg-70Al	1125 ± 46	1123 ± 45
40Mg-60Al	1035 ± 46	1031 ± 45
50Mg-50Mg	1059 ± 51	1057 ± 52

5.3 Aluminum-Lithium System

Only two compositions (6%Li-94%Al and 12%Li-88%Al) of alloys were prepared and tested. Even a small amount of lithium (6%) changes the ignition temperature by about 1280K comparing to that of pure Al (2200K) [Eckhoff, 1991] (Figure 5.8). Ignition was accompanied by a weak, barely visible flash. Photodiode traces indicate small amplitude peaks near the ignition points (Figure 5.9) and at the determination of the ignition temperature using the two techniques described above gave consistent results (Table 5.5).

Variations of heating rate for experiments with Al-Li system were larger comparatively with those for experiments performed with Al-Mg system. Thus measured for Al-Li system experiments heating rate was 1000 ± 200 K/s.

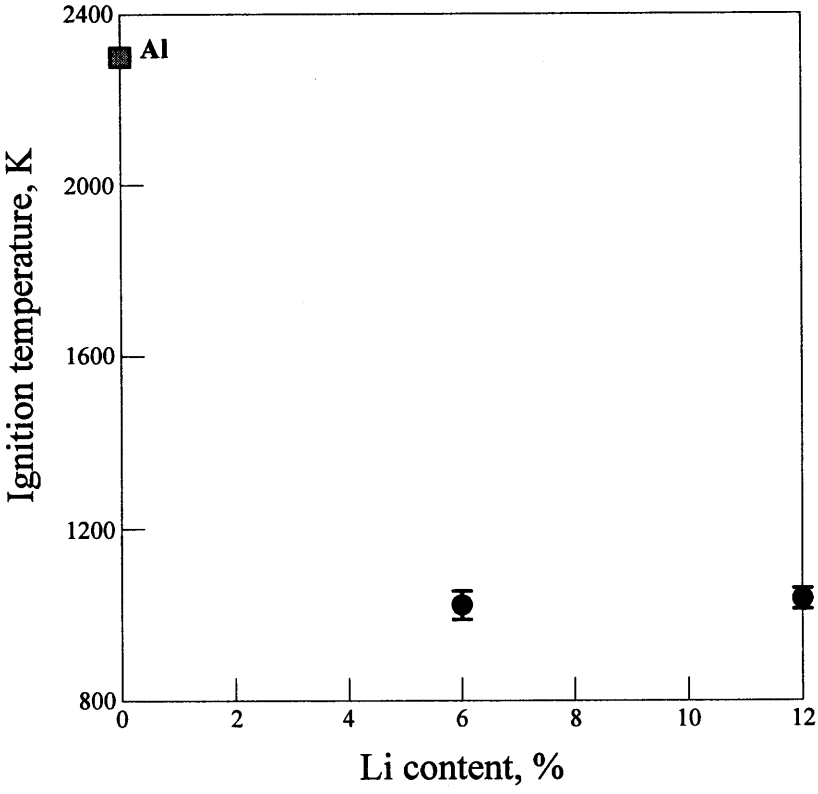

Figure 5.8 Ignition temperature of Al-Li alloys as a function of the Lithium content at a heating rate R=1000 ± 200 K/s.

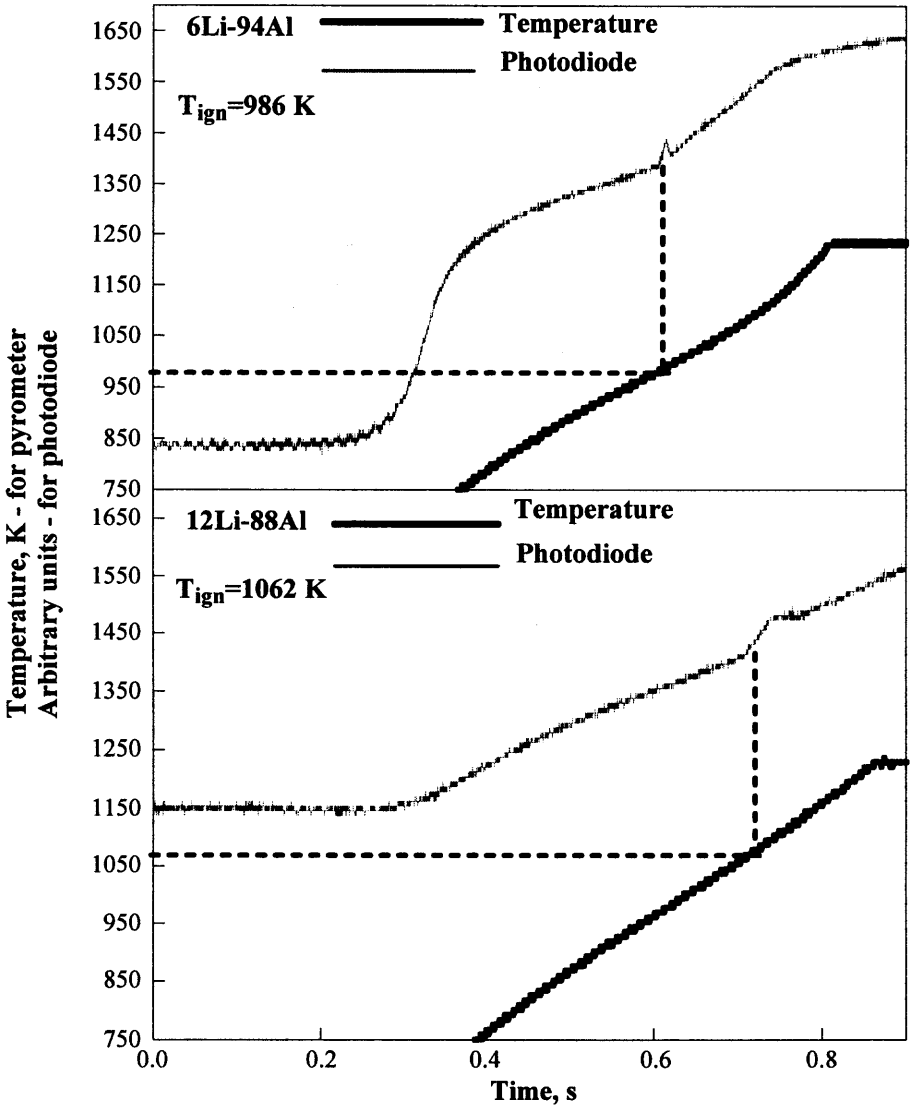

Figure 5.9 Temperature as a function of heating time at a heating rate R=1000 ± 200 K/s for Al-Li alloy system.

Table 5.5 Ignition Temperatures Determined by Two Methods (Section 3.5.2) at a Heating Rate R=1000 ± 200 K/s for Al-Li Alloys(10 repeats for each alloy)

Alloy	Ignition temperature, determined by 1-st method, K	Ignition temperature, determined by 2-nd method, K
6Li-94Al	1031 ± 40	1023 ± 33
12Mg-88Al	1045 ± 24	1038 ± 34

5.4 Ti-B System

Ignition of Ti-B system alloys was qualitatively different as compared to alloys of other systems described above. Observed ignition occurred at a much lower temperature, occurred faster, and was accompanying by a very bright flash, especially for the alloys with higher Ti contents. Sometimes several sparks, one after another, were observed that corresponded to sequential ignition of several particles or particle agglomerates on the filament. Thus, several peaks were often observed on the recorded photodiode traces. Traces of ignition at a heating rate of R=175 ± 40 K/s are shown in Figure 5.10. As ignition temperatures were low for Ti-B system heating rate was calculated on the temperature range from about 670 K, which is a lower limit of detection for used in the study pyrometer, up to ignition temperature. In addition, for Ti-B system experiments were observed different levels of heating rates variations, comparatively with other alloys experiments. At this heating rate, 50%Ti-50%B alloy was ignited at the temperature which was under the limit of the pyrometer detection. For 10%Ti-90%B and 20%Ti-80%B alloys ignition peaks observed on the photodiode traces did not have a sharp front. It caused a discrepancy in ignition temperatures determined by two methods described in Section 3.5.2 (Table 5.6).

Peaks observed on the pyrometer traces for 30%Ti-70%B and 40%Ti-60%B were caused by a very high intensity radiation during the ignition, which affected the pyrometer reading.

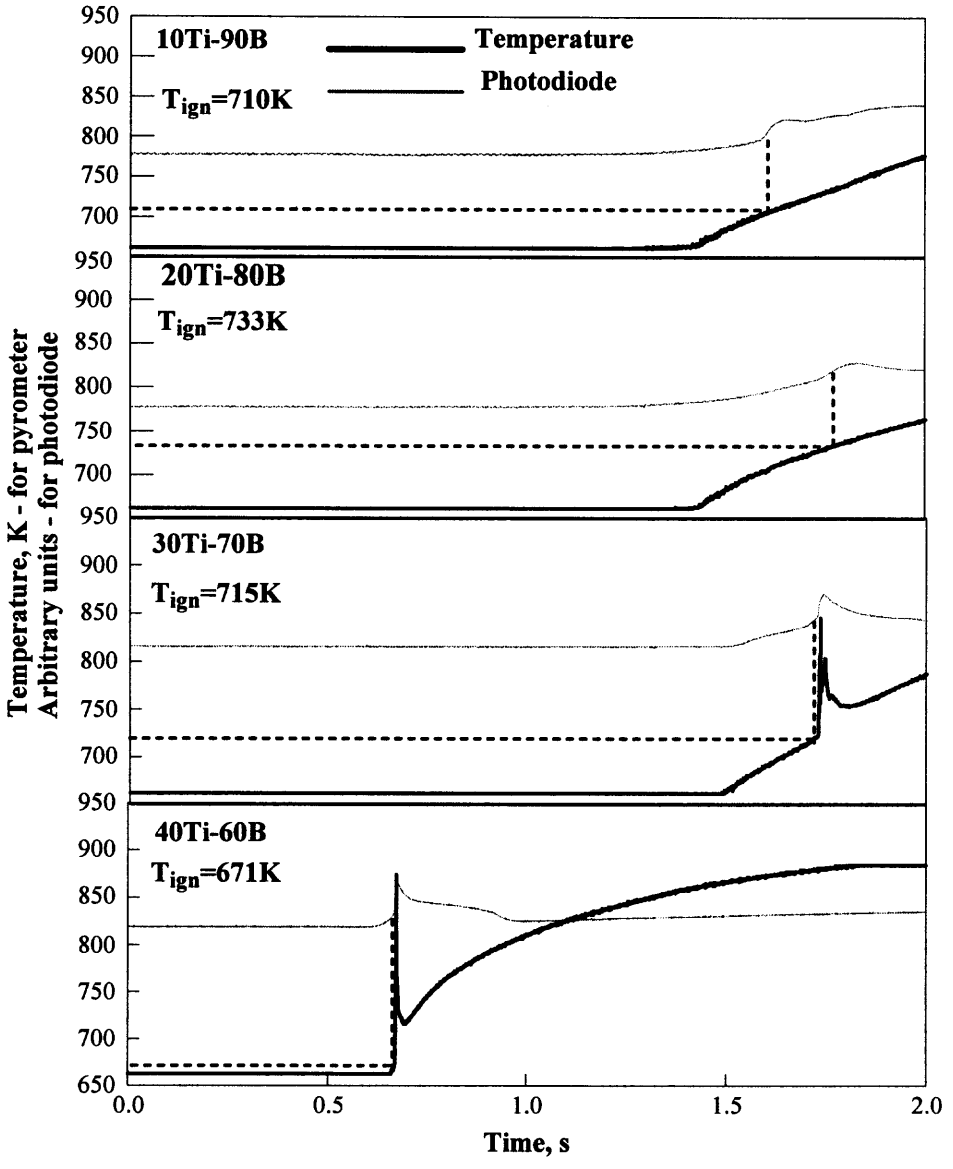

Figure 5.10 Temperature as a function of the heating time at a heating rate R=175 ± 40 K/s for the Ti-B alloy system.

Table 5.6 Ignition Temperatures Determined by Two methods (Section 3.5.2) at a Heating Rate R=175 ± 40 K/s for B-Ti Alloys (10 repeats for each alloy)

Annealed Alloys	Ignition temperature, determined by 1-st method, K	Ignition temperature, determined by 2-nd method, K
10Ti-90B	728 ± 24	726 ± 26
20Ti-80B	720 ± 13	717 ± 12
30Ti-70B	696 ± 24	693 ± 24
40Ti-60B	676 ± 22	674 ± 23

Ignition traces for alloys at heating rates of R=1300 ± 500 K/s and R=5100 ± 1200 K/s are presented in Figure 5.11 and Figure 5.12. Due to scope card triggering problems the trace for 40%Ti-60%B (Figure 5.11) was shifted on 0.09 seconds. For 50%Ti-50%B alloys peaks observed on photodiode traces have a very sharp front and relatively high amplitude. Sensitivity of the photodiode is limited and at a low temperature and fast ignition, the pre-ignition radiation was not detectable. It was also observed that sharp, saturated peaks on the photodiode traces e.g. in Figure 5.11 corresponded to a burning process and not to ignition. However, the time between these two events was so short that the error in the determination of the ignition temperature was negligibly small. In such cases, ignition temperature, determined by two methods described in Section 3.5.2 were the same (Table 5.7, Table 5.8). Observed sharp small peaks on the pyrometer traces (Figure 5.12) are affected by very bright ignition of the powder adjacent to the pyrometer focusing point.

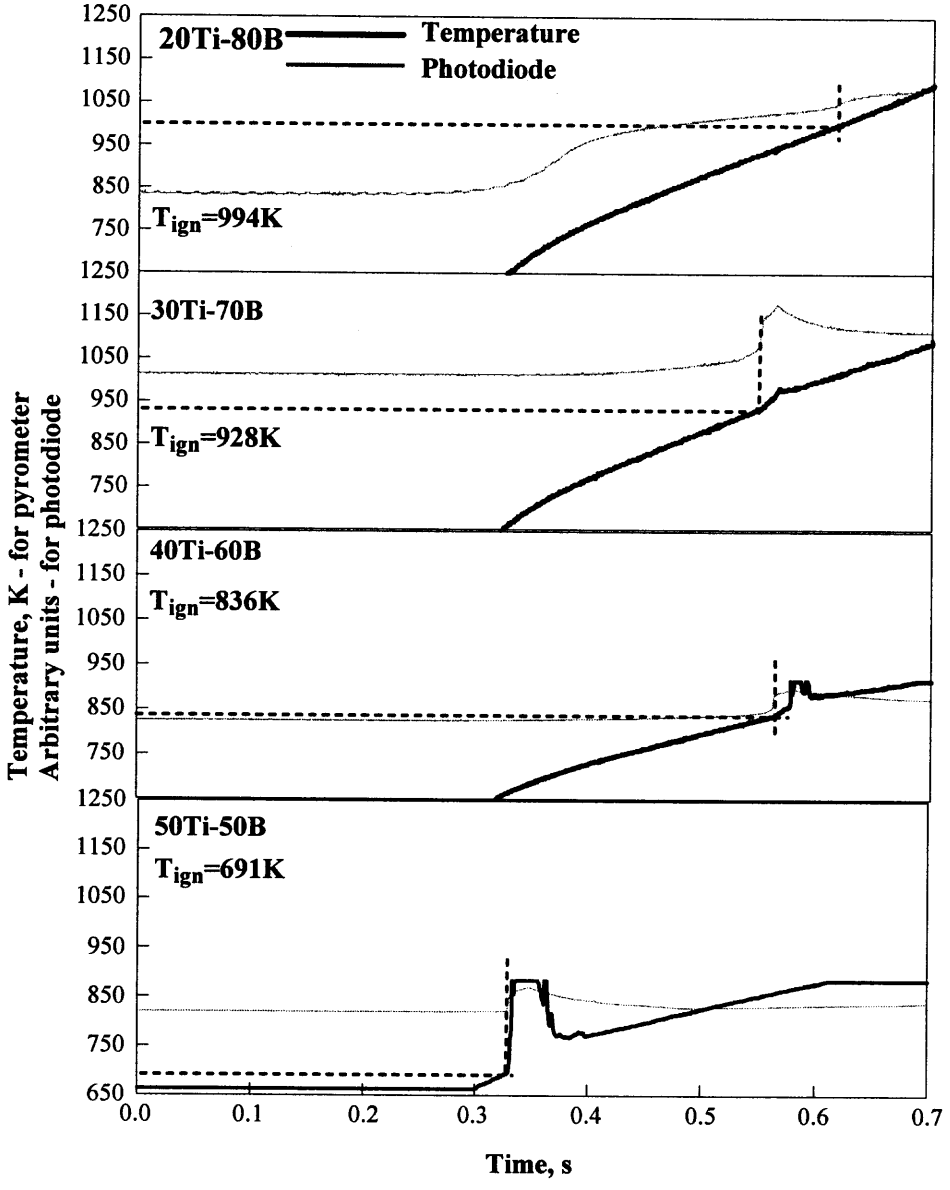

Figure 5.11 Temperature as a function of the heating time at a heating rate R=1300 ± 500 K/s for Ti-B alloy system.

Table 5.7 Ignition Temperatures Determined by Two Methods (Section 3.5.2) at a Heating Rate R=1300 ± 500 K/s for B-Ti Alloys (10 repeats for each alloy)

Annealed Alloys	Ignition temperature, determined by 1-st method, K	Ignition temperature, determined by 2-nd method, K
20Ti-80B	971 ± 52	963 ± 50
30Ti-70B	915 ± 46	906 ± 45
40Ti-60B	809 ± 55	801 ± 53
50Ti-50B	702 ± 36	702 ± 36

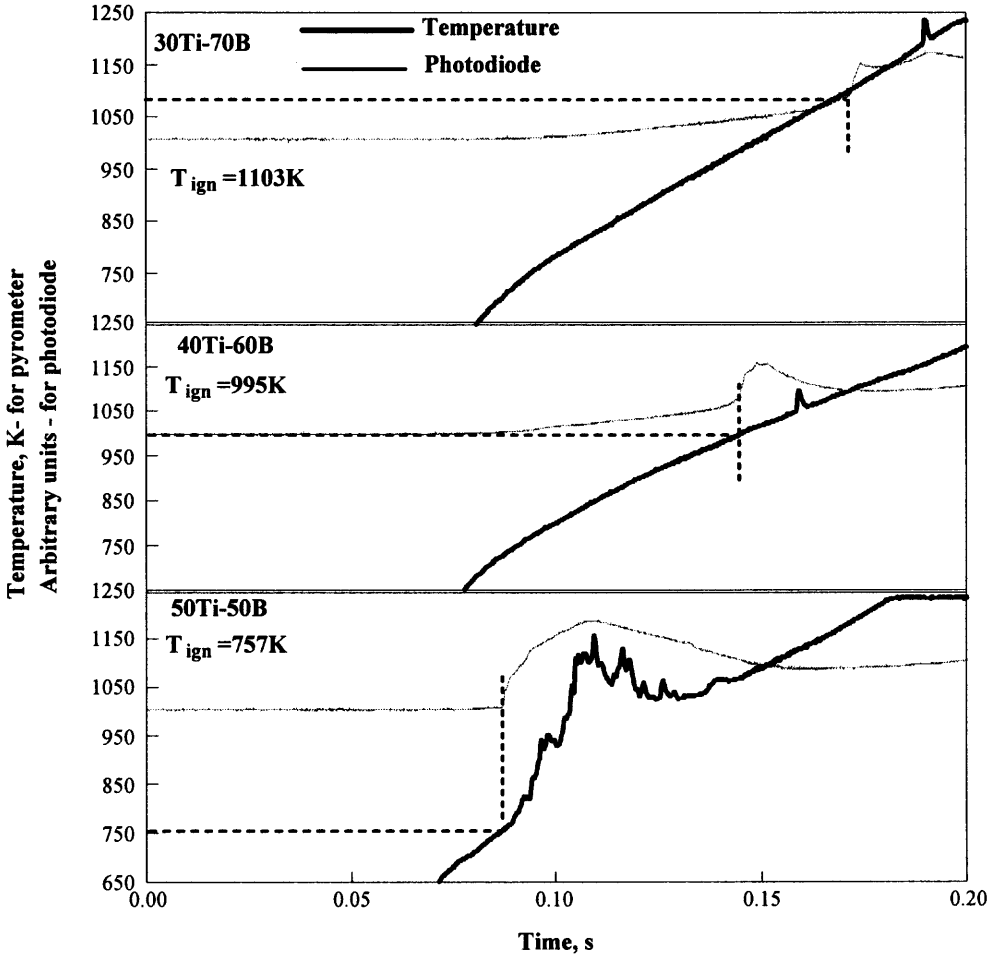

Figure 5.12 Temperature as a function of the heating time at heating rate R=5100 ± 1200 K/s for Ti-B alloy system.

Table 5.8 Ignition Temperatures Determined by Two Methods (Section 3.5.2) at a Heating Rate R=5100 ± 1200 K/s for B-Ti Alloys (10 repeats for each alloy)

Annealed Alloys	Ignition temperature, determined by 1-st method, K	Ignition temperature, determined by 2-nd method, K
30Ti-70B	1113 ± 67	1106 ± 69
40Ti-60B	1003 ± 90	991 ± 88
50Ti-50B	751 ± 18	750 ± 17

It was observed that at higher Ti content in Ti-B alloys the ignition temperatures decreased. Generally, it is suggested that the Ti-B system is also useful for many HEDM. An applications increase in the heating rate had the same qualitative effect on the ignition temperature as for the Al-Mg system alloys: at higher heating rates ignition temperatures were higher (Figure 5.13).

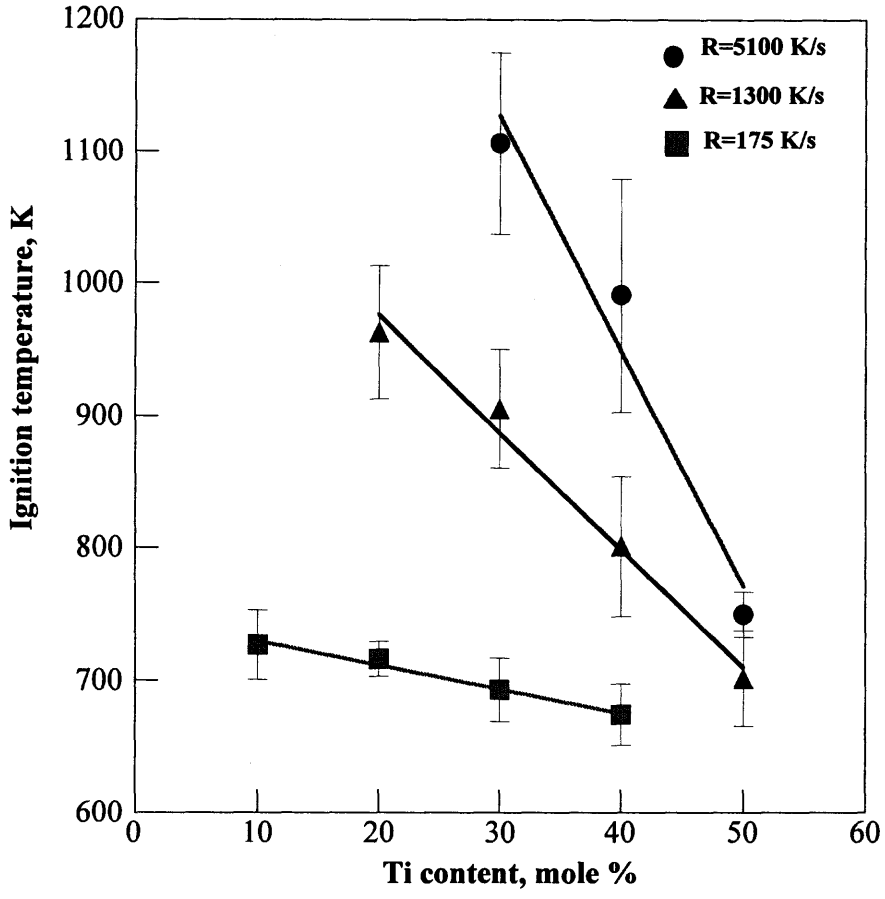

Figure 5.13 Ignition temperatures of Ti-B alloys at the average heating rates of R=175 K/s, R=1300 K/s and R=5100 K/s.

Mechanical alloys of Al with 10%-25% of alloying elements, such as Zr, C, and Ti were also tested. Because the ignition temperatures of these alloys were expected to be high, the experiments were performed with a thin graphite rod as a filament at average heating rate of R=1100 K/s and the temperatures were measured by video technique. Obtained results showed that ignition temperatures of these alloys were lower compared to that of pure aluminum (Figure 5.14) but not as low as for the Al-Mg system alloys. It can be generally suggested that further studies of various aluminum-based alloys are of interest and should carried out in the future.

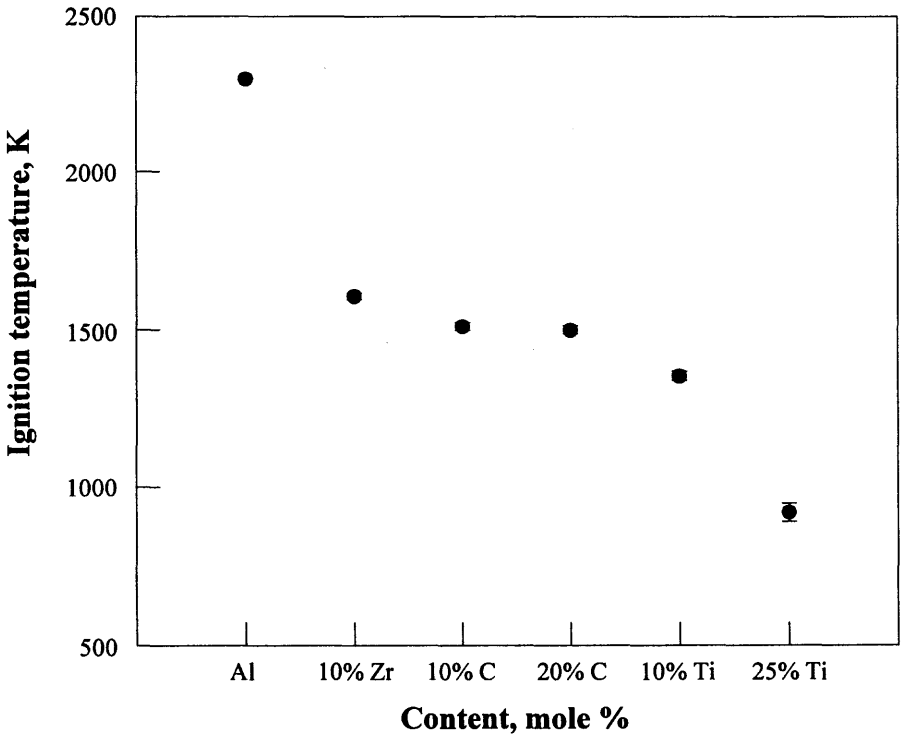

Figure 5.14 Ignition temperatures of different aluminum-based alloys at the average heating rate of R=1100 K/s. Aluminum ignition temperature from [Eckhoff, 1991] is also shown for comparison.

5.5 Ignition of Pure Metals

In a series of additional experiments, several pure metals were ignited at three different heating rates. While ten experiments for each metal were performed at low, medium, and high heating rates, the average values of heating rates were different for each specific metal. Ignition temperatures for Zr, Mg and Ti were found to be higher at increasing heating rates as shown in Figures 5.15-5.17.

These experiments were aimed to provide experimental data for verification of a theoretical metal ignition model being developed in our group [Trunov and Dreizin, paper in preparation].

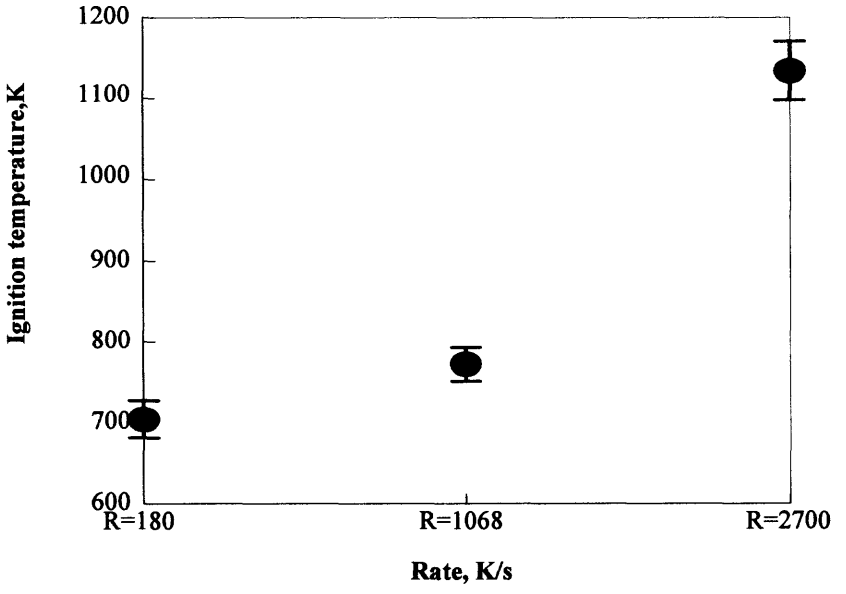

Figure 5.15 Ignition temperatures of zirconium at different heating rates.

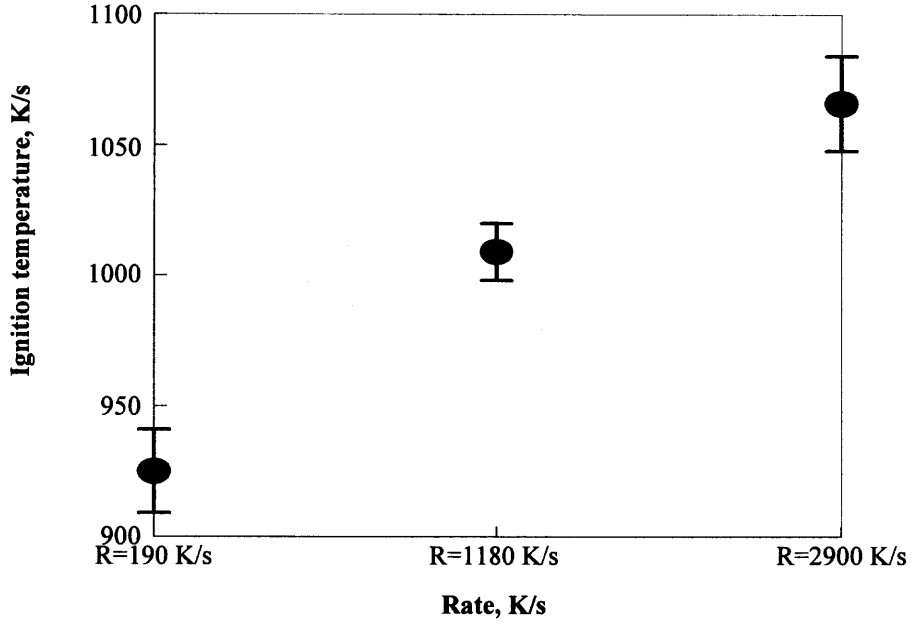

Figure 5.16 Ignition temperatures of magnesium at different heating rates.

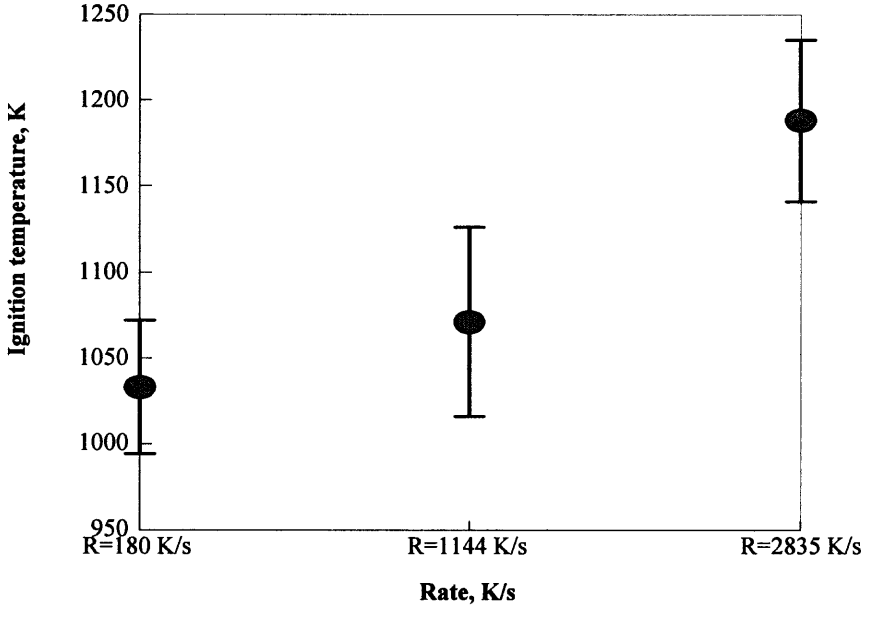

Figure 5.17 Ignition temperatures of titanium at different heating rates.

CHAPTER 6

CONCLUSIONS

Experimental study of ignition of different mechanical alloys and pure metals was performed using video and pyrometer technique. Ignition temperatures were measured using electrically heated filament at three different heating rates (175 - 5100 K/s). A video technique was chosen for ignition temperature measurements for alloys, which ignite at higher temperatures (> 1200 K) and infrared pyrometer technique was used for alloys with lower ignition temperatures. Nickel- Chromium wire and carbon rod served as heated substrates for ignition experiments depending on temperature of ignition. Set of different liquids were used for wetting of powder to produce an adherent coating. Influence of different liquids on ignition temperature of alloys is studied.

Two different methods of ignition moment determination from the photodiode traces are proposed. These methods produce results that are consistent between themselves. Following the same procedure of the temperature determination for different alloys, it was shown that even a small addition of solute elements provides significant decrease in the measured ignition temperatures for both Al-Mg and B-Ti systems.

Annealed alloys were tested on ignition and compared with ignition of "as prepared" mechanical alloys. Difference in the measured ignition temperatures was negligible.

It was observed that for higher heating rate temperature of ignition is higher for all investigated powders. Average ignition temperatures for alloy with small magnesium content (e.g. 20Mg-80Al) at a heating rate of 175 K/s are close to 1018 K, at the rate of

1300 K/s ignition temperature is 1139 K, and the rate of 5100 K/s the temperature is 1162K. The difference in temperatures is relatively large (123 K) between the low and medium heating rate, but only moderate between the medium and fast heating rates, ~ 23 K. For alloys with high magnesium contents (e.g., 50Mg-50Al) at low heating rate (175 K/s) the ignition temperature is 967 K. At a higher rate, 1300 K/s, the ignition temperature increases by 74K (T=1041 K), and at the highest heating rate tested, 5100 K/s, the temperature increases by 50 K (T=1091 K). These results are in qualitative agreement with a theoretical model [Trunov and Dreizin, paper in preparation] suggested for this ignition process. The model describes ignition as a result of a heterogeneous reaction on the particle surface and explains the experimentally observed effect of the heating rate on ignition temperature.

Ti-B alloys ignite at much lower temperatures. For a small titanium content (20Ti-80B) and a heating rate of 175 K/s, the average ignition temperature is 717 K, at the medium heating rate, 1300 K/s, the ignition temperature increases by 246 K (T=963K). For the 50B-50Ti alloys and a low heating rate of 175 K/s, the ignition temperature is 674 K. At a higher heating rate, 1300 K/s, the ignition temperature is 702K, and at the highest tested rate of 5100 K/s, the ignition temperature is 750K.

Al-Li alloys system was investigated at only at the medium heating rate. Alloys with small lithium contents have average ignition temperature nearly 1030 K. Alloys with small contents (10%) of other additives (Zr, Ti, C) have ignition temperature around 1500 K.

APPENDIX

SCOPE CARD CALIBRATION EQUATIONS

Sensitivity of scope card during measurements:

2 volts per division

$$Temperature(K) = 34.656 \times pyrom.sygnal,(a.u.) - 3554.0$$

$$Voltage(V) = 0.059837 \times pyrom.sygnal(a.u.) - 7.4087$$

$$Temperature(K) = 579.17 \times Voltage(V) + 736.88$$

1 volt per division

$$Temperature(K) = 17.166 \times pyrom.sygnal(a.u.) - 1323.2$$

$$Voltage(V) = 0.029852 \times pyrom.sygnal(a.u.) - 3.6551$$

$$Temperature(K) = 575.04 \times Voltage(V) + 778.61$$

0.5 volt per division

$$Temperature(K) = 8.3990 \times pyrom.sygnal(a.u.) - 248.41$$

$$Voltage(V) = 0.015501 \times pyrom.sygnal(a.u.) - 2.0040$$

$$Temperature(K) = 541.84 \times Voltage(V) + 837.44$$

0.2 volt per division

$$Temperature(K) = 3.3225 \times pyrom.sygnal(a.u.) + 396.67$$

$$Voltage(V) = 0.0060773 \times pyrom.sygnal(a.u.) - 0.77657$$

$Temperature(K) = 389.11 \times Voltage(V) + 816.34$ (for temperatures< 730K)

$Temperatur\ e(K) = 331.34 \times Voltage\ (V) + 803.15$ (for temperatures<774K and >730K)

$Temperature(K) = 547.45 \times Voltage(V) + 821.31$ (for temperatures>774K)

0.1 volt per division

$$Temperature(K) = 1.2220 \times pyrom.sygnal(a.u.) + 604.68$$

$$Voltage(V) = 0.0029806 \times pyrom.sygnal(a.u.) - 0.36352$$

$$Temperature(K) = 409.987 \times Voltage(V) + 753.72$$

Temperature as function of voltage has to be the same for any setting of volts per division. First four setting equations differ from each other slightly, probably because of experimental uncertainties in focusing of pyrometer on the black body radiator. Coefficients in the last equation (0.1 volt per division setting) is significantly by different due to signal saturation problem at high temperature. Thus calibration for 0.1 volt per division sensitivity was made at temperature range different from all other sensitivity cases.

REFERENCES

1. R. K. Eckhoff, *Dust Explosions in the process industries*, Butterworth- Henemann, Oxford, England, pp. 276-375, (1991).

2. E. L. Dreizin, Phase Changes in Metal Combustion, *Progress in Energy and Combustion Science*, vol. 26 (1), pp. 57-78, (2000).

3. E. L. Dreizin, D. G. Keil, W. Felder and E. P. Vicenzi, Phase Changes in Boron Ignition and Combustion, *Combustion and Flame*, vol. 119 pp. 272-290, (1999).

4. Y. L. Shoshin, R. S. Mudryy, and E. L. Dreizin, Preparation and Characterization of Energetic Al-Mg mechanical alloy powders, *Combustion and Flame*, vol. 128, pp. 259-269, (2002).

5. R. C. Weast, Handbook of Chemistry and Physics, 61st ed., Boca Raton, FL, CRC Press, pp. E-398 to E-399, (1981).

6. M. A. Trunov and E. L. Dreizin, Theoretical study of ignition of mechanical alloy and pure metal powders, paper in preparation.